

and BTT the peaks at $2\theta = 48.8^\circ$ were associated to Nb_2O_5 (110) and the peaks at $2\theta = 54.4^\circ$ to Nb_2O_5 (102) [28,30]. According to Liu et al. 2016 [30], the peaks showed in samples ATT and BTT at $2\theta = 57.3^\circ$ and $2\theta = 68.4^\circ$ can be associated to Nb_2O_5 . Chan et al. 2017 [31] performed XRD analyses on heat treated niobium up to 500°C and found peaks in DRX 27° , 48° and 55° which were identified as Nb_2O_5 of pseudo-hexagonal crystal structure; in addition, these same authors found peaks around 60° and 70° indicated as Nb_2O_5 of distorted octahedral structure. Pseudo-hexagonal structure of Nb_2O_5 was also observed in the XRD results for the heat-treated samples. The anodized samples without heat treatment showed an amorphous oxide layer. The XRD results indicated that independently of the fluoride concentration in the anodization bath, the heat treatment promoted the formation of crystal oxide on both anodized surfaces.

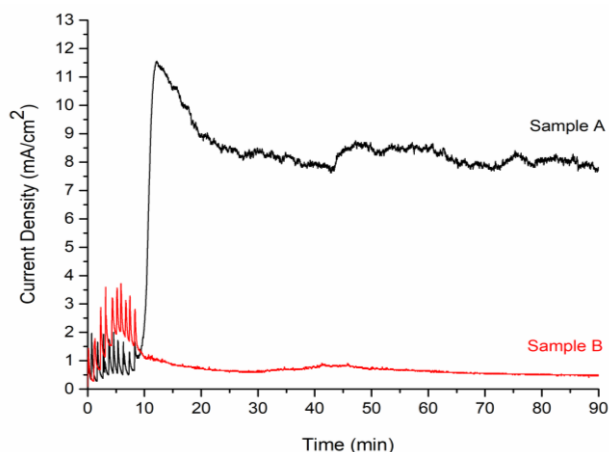


Fig. 1. Transients of current density of the anodized samples.

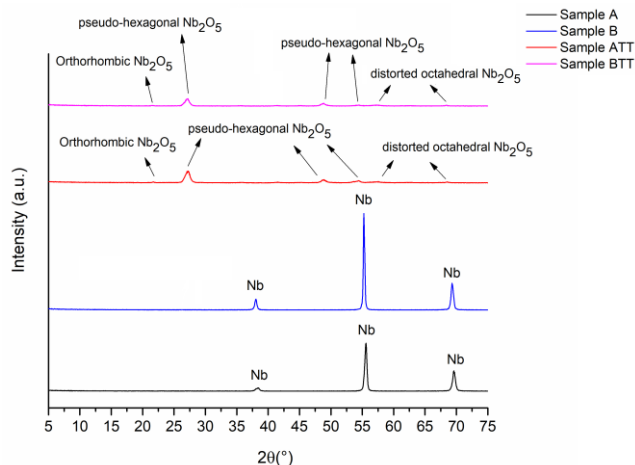


Fig. 2. XRD results of the anodized samples and anodized samples with heat treatment at 450°C ($2^\circ\text{C}/\text{min}$) for 60 minutes.

Figure 3 shows the FEG-SEM images of the anodized niobium that were obtained at different fluoride concentration (Sample A and Sample B) and anodized niobium with heat treatment at 450°C ($2^\circ\text{C}/\text{min}$), 60 min, (Sample ATT and Sample BTT). Sample with low fluoride concentration (Sample A) showed a nanoporous morphology similar to nanotubes; it is in agreement with the current transient (Figure 1), since the variation of the anodic dissolution and the oxide thickening competition promotes the formation of a porous texture [32]. Meanwhile, increasing of the fluoride concentration

contributes to a disordered surface. In relation to heat treated samples, no difference between both morphologies was observed. In both sample ATT and BTT the morphology showed a brittle oxide layer independently of the fluoride concentration. It shows that different fluoride concentrations in the anodization bath had an effect on the morphology of the niobium samples after anodizing process, but with the heat treatment this difference in morphology is no so perceptible; it made the morphology of the surfaces very similar.

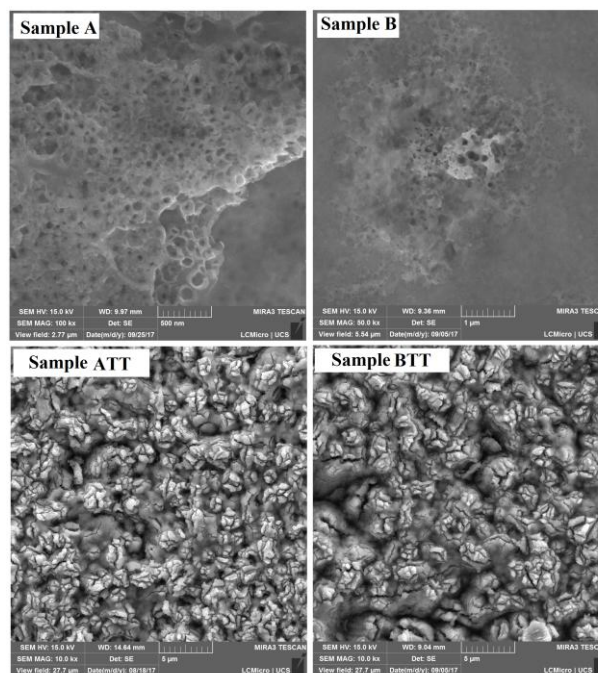


Fig. 3. FEG-SEM images of the anodized niobium samples (Samples A and B) and anodized samples after heat treatment at 450°C ($2^\circ\text{C}/\text{min}$), 60 min.

The best photoelectrochemical performance (greater photocurrent density values) within the electrochemical spectrum of the water reduction reaction for hydrogen production was obtained for sample ATT in clear region (with light) as showed in Fig. 4.

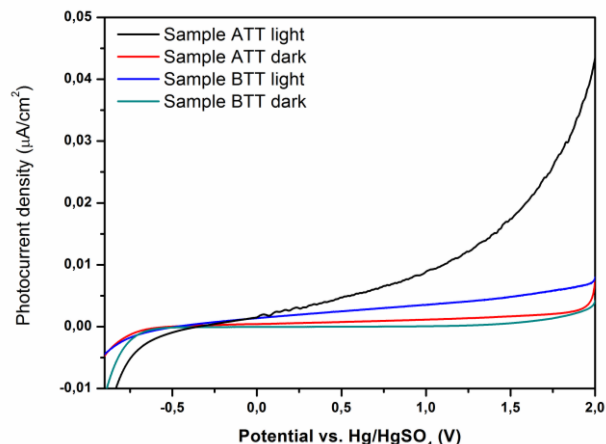


Fig. 4. Linear-sweep voltammograms of anodized niobium electrodes in different fluoride concentration with heat treatment at 450°C ($2^\circ\text{C}/\text{min}$), 60 min, in dark and under illumination. Scan rate is $10\text{ mV}/\text{s}$ and supporting electrolyte is $0,1\text{ M Na}_2\text{SO}_4$.

